Synthesis and Characterization of 2D-D-π-A-Type Organic Dyes Bearing Bis(3,6-di-tert-butylcarbazol-9-ylphenyl)aniline as Donor Moiety for Dye-Sensitized Solar Cells

ARTICLE *in* EUROPEAN JOURNAL OF ORGANIC CHEMISTRY · MAY 2013

Impact Factor: 3.07 · DOI: 10.1002/ejoc.201201479

EurJOC European Journal of Organic Chemistry

DOI: 10.1002/ejoc.201201479

Synthesis and Characterization of 2D-D-π-A-Type Organic Dyes Bearing Bis(3,6-di-*tert*-butylcarbazol-9-ylphenyl)aniline as Donor Moiety for Dye-Sensitized Solar Cells

Tanika Khanasa,[a] Nittaya Jantasing,[a] Somphob Morada,[a] Nararak Leesakul,[b] Ruangchai Tarsang,[a] Supawadee Namuangruk,[c] Tinnagon Kaewin,[a] Siriporn Jungsuttiwong,[a] Taweesak Sudyoadsuk,[a] and Vinich Promarak*[d]

Keywords: Donor–acceptor systems / Dyes / Sensitizers / Conjugation

A series of novel 2D-D-π-A-type organic dyes, namely CCTTnA (n = 1–3), bearing bis(3,6-di-*tert*-butylcarbazol-9-ylphenyl)aniline as an electron-donor moiety (2D-D), oligothiophene segments with a number of thiophene units from one to three units as π-conjugated spacers (π), and cyanoacrylic acid as the electron acceptor (A) were synthesized and characterized as dye sensitizers for dye-sensitized solar cells (DSSCs). These compounds exhibit high thermal and electrochemical stability. Detailed investigations of these dyes reveal that both peripheral carbazole donors (2D) have beneficial influence on the red-shifted absorption spectrum of the dye in solution and dye adsorbed on TiO_2 film, and the broadening of the incident monochromatic photon-to-current conversion efficiency (IPCE) spectra of the DSSCs, leading to enhanced energy conversion efficiency (η). Among these dyes, CCTT3A shows the best photovoltaic performance, and a maximal incident monochromatic photon-to-current conversion efficiency (IPCE) value of 80%, a short-circuit photocurrent density (J_{sc}) of 9.98 mA cm^{-2}, open-circuit voltage (V_{oc}) of 0.70 V, and fill factor (FF) of 0.67, corresponding to an overall conversion efficiency η of 4.6% were achieved. This work suggests that organic dyes based on this type of donor moiety or donor molecular architecture are promising candidates for improved performance DSSCs.

Introduction

Since the report by O'Reagan and Grätzel in 1991 on dye-sensitized solar cells (DSSCs) with dramatically increased light harvesting efficiency,[1] this type of solar cell has attracted considerable and sustained attention because it offers the possibility of low-cost conversion of photoenergy.[2] To date, DSSCs with a validated efficiency record of more than 11% have been obtained with Ru complexes such as the black dye.[3] More recently, a DSSC submodule of 17 cm^2 consisting of eight parallel cells with a conversion efficiency of more than 9.9% was fabricated by Sony.[3] Although there is still room for improvement of the efficiency of Ru-based DSSCs,[4] Ru dyes are nevertheless costly, difficult to attain, and normally have only moderate absorption intensity.[5] Enormous effort is also being dedicated to the development of new and efficient dyes that are suitable with respect to their modest cost, ease of synthesis and modification, large molar extinction coefficient, and long-term stability. Organic dyes meet all these criteria. Thus, there have been remarkable developments in organic dye-based DSSCs in recent years,[6] and efficiencies exceeding 10% have been achieved by using dyes that have broad, red-shifted, and intense spectral absorption in the visible light region.[7] Although remarkable progress has been made in the development of organic dyes as sensitizers for DSSCs, their chemical structures still require optimization for further improvement in performance. Most of the developed organic dyes are composed of donor, π-conjugation, and acceptor moieties, thereby forming a D-π-A structure, and broad ranges of conversion efficiencies have been achieved.[6–8] Most of the highly efficient DSSCs based on organic dyes have long π-conjugated spacers between the donor and acceptor, resulting in broad and intense absorption spectra, aromatic amines as donor moieties, a strong electron-withdrawing group (cyanoacrylic acid) as acceptor, and anchoring moieties. However, the introduction of long π-conjugated segments results in rod-like molecules, which can lead to recombination of the electrons to the triiodide and magnify

[a] Center for Organic Electronic and Alternative Energy, Department of Chemistry, Faculty of Science, Ubon Ratchathani University, Ubon Ratchathani 34190, Thailand
[b] Department of Chemistry, Faculty of Science, Prince of Songkhla University, Hat Yai, Songkhla 90110, Thailand
[c] National Nanotechnology Center, 130 Thailand Science Park, Paholyothin Rd., Klong Luang Pathumthani 12120, Thailand
[d] School of Chemistry and Center of Excellence for Innovation in Chemistry, Institute of Science, Suranaree University of Technology, Muang District, Nakhon Ratchasima 30000, Thailand
Fax: +66-44-224648
E-mail: pvinich@sut.ac.th

Supporting information for this article is available on the WWW under http://dx.doi.org/10.1002/ejoc.201201479.

aggregation between molecules.[9] The close π-π aggregation can not only lead to self-quenching and reduction of electron injection into TiO_2, but can also result in instability of the organic dyes due to the formation of excited triplet states and unstable radicals under light irradiation.[10] On the basis of these criteria, recently, organic dyes with 2D-π-A structures have been reported by several groups.[11] Their studies suggest that good performance for organic dyes based on 2D-π-A structure over the simple D-π-A configuration could be achieved by the molecular design.

We anticipated that further improvements could be made by introducing an additional donor moiety into the aromatic amine to form a 2D-D-π-A structure, and envisaged that such architectures would extend the absorption region, enhance the molar extinction coefficient, reduce the tendency to aggregate, and lead to better thermal stability compared with simple D-π-A structures. To this end, we prepared a set of new, simple 2D-D-π-A-type organic dyes. In our design (Figure 1), triphenylamine and carbazole moieties were employed as the aromatic and additional donors, respectively, thereby forming a bis(3,6-di-*tert*-butylcarbazol-9-ylphenyl)aniline donor moiety (2D-D). The cyanoacrylic acid and oligothiophenes were incorporated as acceptor (A) and simple π-spacer (π), respectively. Recently, efficient DSSCs that incorporate various triphenylamine and carbazole-based dyes have been reported, indicating the importance of their further investigation in DSSCs.[12] In addition, it has been found that by incorporating an electron-donor group into the dye molecule, the physical separation of the dye cation from the electrode surface can be increased, which facilitates a high rate of charge separation and collection compared with interfacial charge-recombination processes.[13] Furthermore, the use of triphenylamine and carbazole have aroused great interest because of their excellent hole-transport capability, and their derivatives have become classic hole-transporting materials.[14] Moreover, the bulky, nonplanar structure of this 2D-D moiety may prove to be important for solving the intractable problems associated with close π-π aggregation of the dye molecules. The inclusion of *tert*-butyl substituents can increase the solubility of the dye, and also form a hydrophobic blocking layer on the TiO_2 surface to suppress the approach of iodide/triiodide (I^-/I_3^-) electrolyte to the TiO_2, consequently leading to an improvement in the open-circuit voltage. Herein, we report a detailed synthesis and the physical and photophysical properties of these 2D-D-π-A-type dyes (CCTTnA). Furthermore, their use as dye sensitizers in DSSCs in comparison with N3 dye and D-π-A-type dye (TT2A),[15] having triphenylamine as a donor, are also reported.

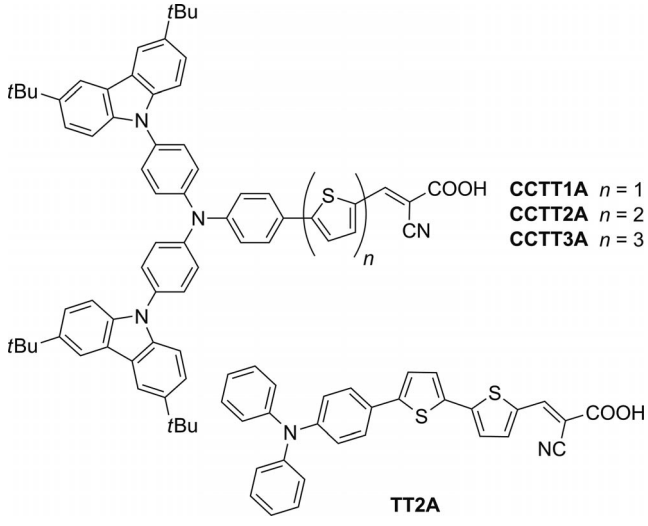

Figure 1. Molecular structures of the designed dyes.

Results and Discussion

Synthesis and Characterization

The dyes were synthesized as outlined in Scheme 1. First, a key intermediate, *N*,*N*-bis[4-(3,6-di-*tert*-butylcarbazol-9-yl)phenyl]-4-iodoaniline (**3**), was synthesized from Ullmann coupling of tri(*p*-iodophenyl)amine (**1**) with 3,6-di-*tert*-butylcarbazole (**2**) obtained from directed iodination of triphenylamine with I_2, and from an alkylation of carbazole with *tert*-butyl chloride, respectively. A stoichiometric reaction of **1** (2 equiv.) and **2** (1 equiv.) under a catalytic system of CuI as catalyst, (±)-*trans*-1,2-diaminocyclohexane as co-catalyst, and K_3PO_4 as base in toluene, afforded intermediate **3** in moderate yield (44%). From **3**, intermediates **5** and **7** were synthesized by using a combination of Suzuki cross-coupling and bromination reactions in an iterative manner. Suzuki cross-coupling reaction with 2-thiophene boronic acid catalyzed by $[Pd(PPh_3)_4]/Na_2CO_3$ (aq.) in tetrahydrofuran (THF) was employed to achieve an increased number of thiophene units in the molecule, whereas bromination with *N*-bromosuccinimide (NBS) in THF selectively introduced a bromo function to the α-position of the terminal thiophene ring, allowing a further Suzuki cross-coupling reaction to be performed. The Suzuki coupling of **3** and **5** with 2-thiophene boronic acid afforded thiophene compounds **4** and **6** in good yields, whereas bromination of **4** and **6** with NBS yielded bromo intermediates **5** and **7** in 91 and 87%, respectively. Subsequent coupling of intermediates **3**, **5** and **7** with 5-formylthiophene-2-boronic acid under the same Suzuki coupling conditions gave **8**, **9**, and **10** in yields of 75, 70, and 60%, respectively. Final Knoevenagel condensation of these aldehydes with cyanoacrylic acid in the presence of a catalytic amount of piperidine in $CHCl_3$ heated at reflux for 18 h gave (*E*)-3-[5-(4-{bis[4-(3,6-di-*tert*-butylcarbazol-9-yl)phenyl]amino}phenyl)thiophen-2-yl]-2-cyanoacrylic acid (CCTT1A), (*E*)-3-[5′-(4-{bis[4-(3,6-di-*tert*-butylcarbazol-9-yl)phenyl]amino}phenyl)-(2,2′-bithiophen)-5-yl]-2-cyanoacrylic acid (CCTT2A) and (*E*)-3-[5′′-(4-{bis[4-(3,6-di-*tert*-butylcarbazol-9-yl)phenyl]amino}-phenyl)-(2,2′:5′,2′′-terthiophen)-5-yl]-2-cyanoacrylic acid (CCTT3A) in yields of 58, 57, and 48%, respectively. All dyes can be crystallized to give intensely colored solids. The colors of these solid products varied from orange to dark-red as the number of thiophene units in the molecule in-

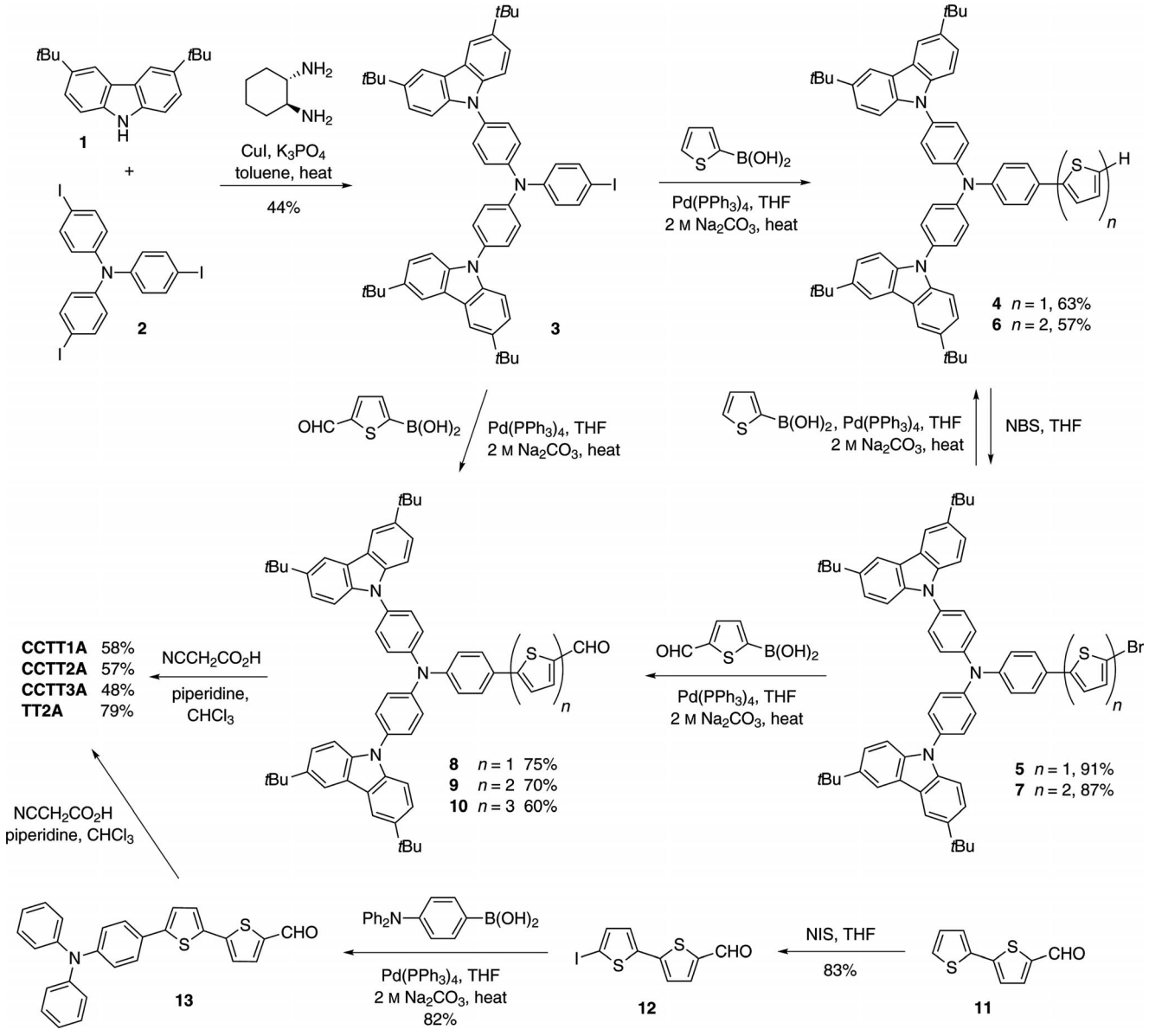

Scheme 1. Synthesis of CCTTnA (n = 1–3) and TT2A dyes.

creased from CCTT1A, CCTT2A to CCTT3A. In the synthesis of (*E*)-3-{5′-[4-(diphenylamino)phenyl]-2,2′-bithiophen-5-yl}-2-cyanoacrylic acid (TT2A), intermediate 2,2′-bithiophene-5-carbaldehyde (**11**) was first selectively iodinated at the α-position of the terminal thiophene ring with NIS in THF to give 5′-iodo-2,2′-bithiophene-5-carbaldehyde (**12**) in 83% yield. Subsequently, Suzuki coupling of **12** with 4-(diphenylamino)phenylboronic acid[16] afforded 5′-[4-(diphenylamino)phenyl]-2,2′-bithiophene-5-carbaldehyde (**13**) in a yield of 82%. Knoevenagel condensation of this aldehyde with cyanoacrylic acid catalyzed by piperidine produced TT2A in 79% yield. The structures of all dye molecules were characterized unambiguously on the basis of FTIR, ^{1}H NMR, and ^{13}C NMR spectroscopy as well as high-resolution mass spectrometry. These compounds show good solubility in organic solvents, presumably as a result of their steric bulk and the presence of *tert*-butyl substituents, allowing dye adsorption on TiO_2 film and fabrication of DSSCs.

Optical Properties

UV/Vis absorption spectra of CCTTnA and TT2A in CH_2Cl_2 are shown in Figure 2 and the characteristic data are summarized in Table 1. The spectra of CCTTnA exhibited three strong absorption bands at 297–298, 330–340, and 455–464 nm, respectively (Figure 2, a). The first and second absorption bands were attributed to localized π-π* transitions of the carbazole and triphenylamine donors (2D-D), respectively. The third band was ascribed to intramolecular charge transfer (ICT) transition from the 2D-D moiety to the cyanoacrylic acid acceptor. This was con-

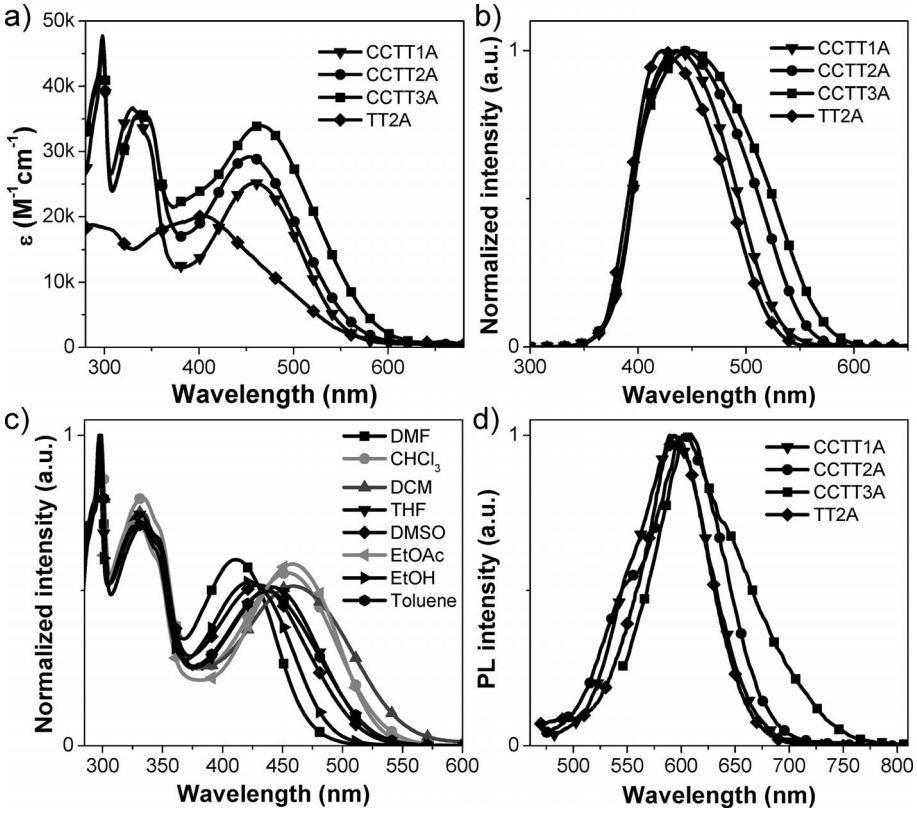

Figure 2. UV/Vis absorption spectra of dyes (a) in CH_2Cl_2 solution and (b) adsorbed on TiO_2 film. (c) UV/Vis absorption spectra of CCTT1A in different solvents. (d) PL spectra of dyes in CH_2Cl_2 solution.

Table 1. Optical, thermal, electrochemical, and electronic properties of the dyes.

Dye	$Abs._{max}$[a] [nm]	ε [$M^{-1}cm^{-1}$]	Abs.[b] [nm]	$Em._{max}$[a] [nm]	τ [ns] (%)[c]	χ^2[c]	$E_{1/2}$ vs. Ag/Ag^+[d] [V]	T_{5d}[e] [°C]	E_g[f] [eV]	E_g cal[g] [eV]	HOMO/LUMO[h] [eV]
CCTT1A	458	25225	436	646	1.14 (74.6)	0.60	–1.61, 0.83, 1.08, 1.40	284	2.25	2.38	–5.22/–2.97
CCTT2A	455	29322	442	658	0.88 (61.0)	0.73	–1.86, 0.81, 1.08, 1.35, 1.50	285	2.21	2.19	–5.20/–2.99
CCTT3A	464	33926	450	672	0.85 (80.5)	1.12	–1.61, 0.78, 0.99, 1.06, 1.31, 1.37	353	2.13	2.08	–5.16/–3.03
TT2A	405	20206	422	651	1.30 (97.6)	0.90	–1.55, 0.92, 1.35	290	2.25	2.38	–5.28/–3.03
N3[19]	530	14500	–	–	–	–	–	–	1.86	1.86	–5.52/–3.84

[a] Absorption and emission measured in CH_2Cl_2 solution. [b] Absorption of the dyes adsorbed on TiO_2 film. [c] Fluorescence lifetime measured in CH_2Cl_2 solution at 25 °C. [d] Measured by CV using a glassy carbon working electrode, Pt counter electrode and Ag/Ag^+ reference electrode with 0.1 M nBu_4NPF_6 as supporting electrolyte in CH_2Cl_2. [e] Measured by TGA at a heating rate of 10 °C/min under N_2. [f] Estimated from the absorption onset: $E_g = 1240/\lambda$. [g] Calculated by at the TDDFT/B3LYP/6-31G (d,p) level. [h] Calculated from oxidation onset potential: HOMO = $-(E_{onset}^{ox} + 4.44)$; LUMO = HOMO – E_g.

firmed by a negative solvatochromic shift, i.e., hypsochromic shift of maximum wavelength (λ_{max}) of the peaks at longer wavelength in more polar solvents, whereas the positions of the first and second absorption bands were nearly independent of solvent polarity (Figure 2, c). The molar extinction coefficients (ε) of the first and second absorption bands of all compounds were nearly identical (ε = 42326 and 33061 $M^{-1}cm^{-1}$, respectively), as they have the same donor. The ε values of the ICT bands of CCTTnA were moderate to high, ranging from 25225 to 33926 $M^{-1}cm^{-1}$. As the number of thiophene units in the molecules increase from CCTT1A, CCTT2A to CCTT3A, the ICT bands showed bathochromic shifts and increased ε values. The absorption spectra and the ε values of conjugated chromophores increase as the degree of conjugation is extended.[17]

Comparison of the absorption spectra and ε values of 2D-D-π-A dyes CCTT1A and CCTT2A to those of (*E*)-3-{5-[4-(diphenylamino)phenyl]thiophen-2-yl}-2-cyanoacrylic acid (λ_{ICT} = 379 nm, ε = 17000 $M^{-1}cm^{-1}$ in $CHCl_3$)[18] and TT2A (λ_{ICT} = 405 nm, ε = 20206 $M^{-1}cm^{-1}$), having simple D-π-A structures, revealed significant bathochromic shifts (50–79 nm) of the ICT peaks and increases in the ε values (1.45–1.48 fold). These results suggest that the use of carbazole as an additional or secondary donor to triphenyl-

amine donor to form a 2D-D-π-A structure dye may be an effective way to bathochromically shift and enhance the ε value of the dye's absorption spectra, which is desirable for harvesting more solar light. Moreover, the ε values of the ICT peaks of these dyes are considerably larger than that of the Ru dye (N3, $\varepsilon_{730\,nm}$ = 14500 $M^{-1}cm^{-1}$),[19] indicating good light harvesting ability. The higher ε values of the dyes allow a correspondingly thinner nanocrystalline film to be used, so avoiding a decrease in the mechanical strength of the film. This is also advantageous for electrolyte diffusion in the film and reduces the possibility of recombination of the light-induced charges during transportation.[20] The absorption spectra of CCTTnA adsorbed on TiO_2 films are shown in Figure 2 (b). The spectra were slightly blueshifted (13–22 nm) compared with spectra measured in CH_2Cl_2. Such a phenomenon is commonly observed in the spectral response of other organic dyes, and may be ascribed to the H-aggregation of the dye molecules on the TiO_2 surface and/or the interaction of the anchoring groups of the dyes with the surface of TiO_2.[21] The fluorescence emission spectra of the dyes in CH_2Cl_2 were redshifted with increasing numbers of thiophene units in the molecule, which was roughly parallel to the trend of the absorption spectra (Figure 2, d). The fluorescence decay curves of the dyes were measured in CH_2Cl_2 at 25 °C and their decay parameters giving the best fit are summarized in Table 1. As the number of thiophene units in the molecule increased from CCTT1A, CCTT2A to CCTT3A, the major relaxation time decreased from 1.14, 0.88 to 0.83 ns, respectively.

Electrochemical and Thermal Properties

The electrochemical properties of the dyes were studied by cyclic voltammetry (CV) in CH_2Cl_2 solution with 0.1 M nBu$_4$NPF$_6$ as a supporting electrolyte. The results are shown in Figure 3 (a) and all data are listed in Table 1. The CV curves of all dyes exhibited multi quasireversible oxidation events and one irreversible reduction process. The reduction wave was attributed to the reduction of the cyanoacrylic acid acceptor moiety, which was in the range of –1.55 to –1.86 V. The first oxidation wave of TT2A agreed with the removal of electrons from the triphenylamine donor to give the corresponding radical cation, whereas those of CCTTnA corresponded to removal of electrons from the peripheral carbazole donor moieties to give the radical cation. The first oxidation potentials of CCTTnA decreased from 0.88, 0.83 to 0.78 V when the number of thiophene units in the molecule or the length of the π-conjugated spacers were increased from CCTT1A, CCTT2A to CCTT3A, respectively, as observed in other oligothiophenes.[22] These values were lower than that of TT2A (0.92 V), indicating the advantage of having peripheral carbazoles as extra donors. The multiple CV scans of CCTTnA revealed identical CV curves, with no additional peak at lower potential on the cathodic scan (E_{pc}) being observed. This indicates that no oxidative coupling at the 3 or 6 positions of the peripheral carbazole, leading to electropolymerization, took place, presumably due to the presence of the 3,6-di-*tert*-butyl groups. This type of electrochemical coupling reaction can be detected in some carbazole derivatives with unsubstituted 3,6-positions[23] and might occur upon charge separation, which hampers the dye regeneration. Therefore, importantly, it is clear that the dyes are electrochemically stable molecules.

The HOMO and LUMO energy levels of the dyes calculated from the onset potential of the CV curves are summarized in Table 1. The HOMO of CCTT1A (–5.22 eV) was lower than those of both CCTT2A (–5.20 eV) and CCTT3A (–5.16 eV), but all were much lower than the redox potential of the I^-/I_3^- couple (–4.8 eV), therefore, dye regeneration should be thermodynamically favorable and should compete efficiently with the recapture of the injected electrons by the dye radical cation. The LUMOs (–2.97 to –3.03 eV) of these dyes calculated from the HOMOs and energy gaps (E_g) estimated from the optical absorption edge were less negative than the conduction band of the TiO_2 electrode (–4.00 eV vs. vacuum)[24] and the LUMO of N3 dye (–3.84 eV).[19] To ensure efficient charge injection, the LUMO level of the dye should be more than 0.3 eV above the conduction band of the TiO_2. Therefore, all dyes have sufficient driving force for electron injection from the excited dyes to the conduction band of TiO_2. As a result,

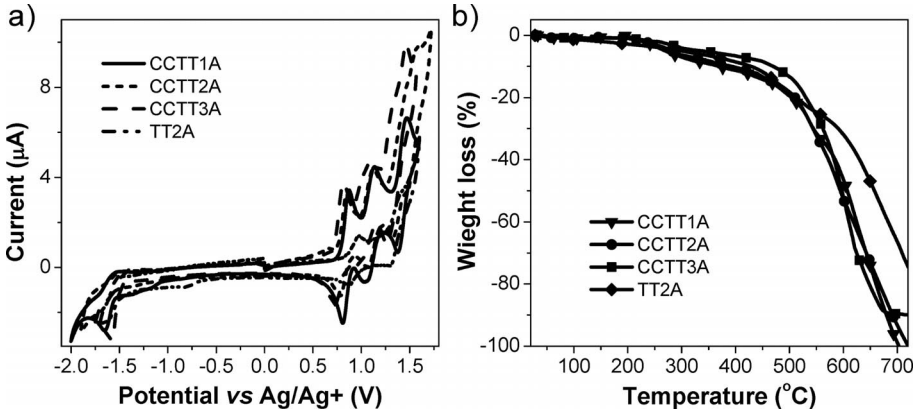

Figure 3. (a) CV curves measured in CH_2Cl_2 solution with nBu$_4$NPF$_6$ as supporting electrolyte at a scan rate of 100 mV/s. (b) TGA thermograms measured at a heating rate of 10 °C/min under N_2.

CCTTnA have sufficient energetic driving force for efficient DSSCs using a nanocrystalline titania photocatalyst and the I^-/I_3^- redox couple. Moreover, having high LUMO potentials, these dyes become very attractive for other metal oxide semiconductors with higher conduction bands than that of TiO_2 such as ZnO, Nb_2O_3, $SrTiO_3$ and their composites[25] to achieve high open-circuit voltage (V_{oc}) DSSCs.

The thermal properties were investigated by thermogravimetric analysis (TGA), and the results suggested that dyes CCTTnA were thermally stable materials, with temperature at 5% weight loss (T_{5d}) well over 285 °C (Figure 3, b). The better thermal stability of the dye is important for the lifetime of the solar cells.[26]

Quantum Chemical Calculations

To gain insight into the geometrical, electronic, and optical structures of these new dyes, quantum chemistry calculations were performed at the TDDFT/B3LYP/6-31G (d,p) level;[27] the results are summarized in Figure 4 and detailed in the Supporting Information. A major factor leading to low conversion efficiencies of many organic dyes in DSSCs is the formation of dye aggregation on the semiconductor surface.[10] We therefore included a bulky donor moiety equipped with two 3,6-di-*tert*-butylcarbazole units connected to a triphenylamine unit to increase the steric bulk of the molecule. The optimized structures of CCTTnA revealed that the dihedral angles formed between carbazole (D1) and phenyl (Ph) planes in all molecules were as large as 54.34–55.63° due to the steric bulk of the structure, which could help to prevent close π-π aggregation effectively between the dye molecules. The noncoplanar geometry can also reduce contact between molecules and enhance their thermal stability.[28] The aromatic rings of the π-conjugated spacers adopted more planar conformations, with the dihedral angles between the benzene and thiophene (T_1) planes ranging from 19.60 to 22.80°, and the thiophene (T_1) and thiophene (T_2, T_3) planes (CCTT2A and CCTT3A) ranging from 4.23 to 10.54°, whereas the thiophene (T_3) and acrylic acid (A) planes were nearly coplanar (dihedral angle of less than 0.15°). This suggests that π-electrons from the donor moiety can delocalize effectively to the acceptor moiety, which can subsequently transfer to the conduction band of TiO_2.

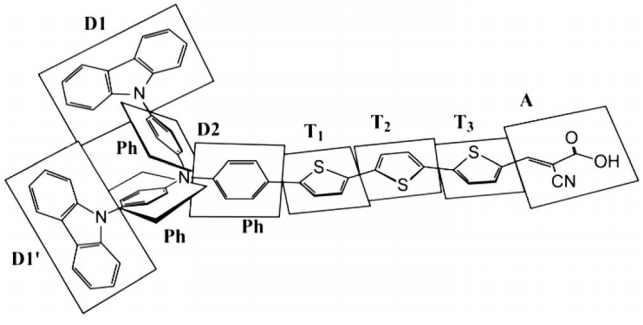

Figure 4. Schematic views of the ground state structures for CCT3A.

The molecular orbital distribution is very important in determining the charge-separated states of organic dyes. The electron distributions of the HOMO and LUMO of CCTTnA and TT2A are shown in Figure 5 and in the Supporting Information. To create an efficient charge-transfer transition, the HOMO must be localized on the donor unit and the LUMO on the acceptor unit.[29] The HOMOs of these compounds are calculated to delocalize over the donor moiety. In CCTTnA dyes, the major contribution of the donor moiety comes from both triphenylamine and each peripheral carbazole. The LUMOs are delocalized across the oligothiophene groups and cyanoacrylic acid acceptor. The results indicate that the distribution of the HOMO and LUMO of all dyes is well-separated, suggesting that the HOMO–LUMO transition and can be considered as an ICT transition. The lowest transition ($S_0 \rightarrow S_1$; > 93% HOMO→LUMO) of CCTTnA dyes corresponds to a charge-transfer excitation from the carbazole-triphenylamine donor to the oligothiophene π-spacer and cyanoacrylic acid acceptor (see the Supporting Information). The S_2 transition state ($S_0 \rightarrow S_2$; > 88%) is related to a HOMO–1→LUMO transition and has a charge shift mainly from the two peripheral carbazole moieties to the oligothiophene π-spacer and cyanoacrylic acid acceptor, which is reflected in the molecular orbital involved in the transition as well as in the low oscillator strength due to the long-range charge shift. For the S_3 transition state ($S_0 \rightarrow S_3$; > 88% HOMO–2→LUMO), a charge shift mainly originates from the donor moiety and oligothiophene π-spacer to the oligothiophene π-spacer and cyanoacrylic acid acceptor with moderate to high oscillator strengths. This means that these additional carbazole donor units may cause a cascade effect that aids charge separation. Therefore, it is believed that

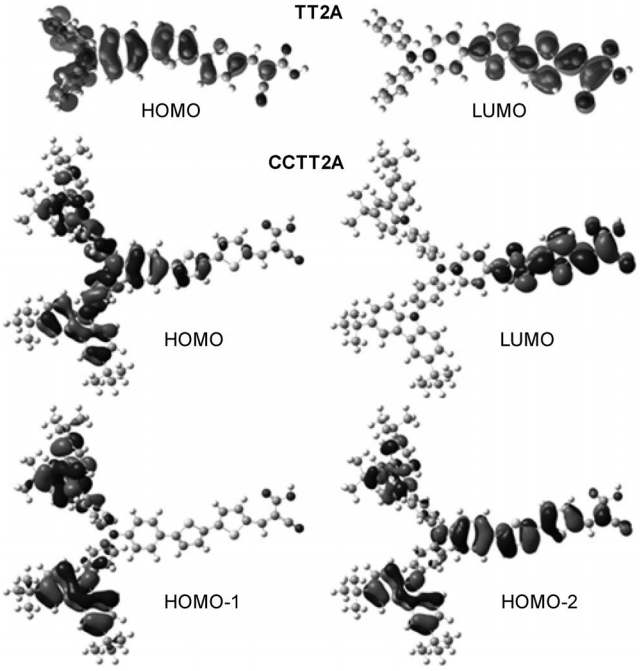

Figure 5. The HOMO and LUMO orbitals of **TT2A** (top) and **CCTT2A** (bottom).

both $S_0 \rightarrow S_2$ and $S_0 \rightarrow S_3$ transitions can also inject electrons either directly into the conduction band of the TiO_2, or indirectly through internal conversion to $S_0 \rightarrow S_1$, which would result in an improved short-circuit current (J_{sc}) of DSSCs. As expected, the calculated HOMOs, LUMOs, and energy gaps (E_g cal) of CCTTnA decrease when the number of thiophene units in the molecule is increased, in agreement with experimental absorption spectra and electrochemical results. These E_g cal values were slightly higher than those estimated from the optical absorption edge (E_g) (Table 1), however, the orbital energy difference between HOMO and LUMO is still an approximate estimation of the transition energy because the transition energy also contains significant contributions from some two-electron integrals. The real situation is that an accurate description of the lowest singlet excited state requires a linear combination of a number of excited configurations.

Dye Adsorption on TiO_2

The performance of a DSSC is not only based on the absorption of the harvesting dye but also on the total amount of dye present. Therefore, dye uptake was determined by using spectrophotometric measurements of UV/Vis absorption according to a reported method.[30] Figure 6 (a) shows the dye uptake profiles as a function of time for CCTTnA and TT2A (see also the Supporting Information). In all cases, dye uptake markedly increased at the beginning until it reached a plateau at about 30 h. These profiles are typical for organic adsorbates into nanoporous inorganic matrices.[31] It was found that, at the equilibrium maximum, uptakes of each dye were 44.44×10^{15}, 50.65×10^{15}, 53.90×10^{15} and 83.14×10^{15} molecules cm^{-2} for CCTT1A, CCTT2A, CCTT3A and TT2A, respectively (Table 2). The lower dye uptake of CCT1A on the TiO_2 film compared to others can be rationalized by the steric hindrance of the donor moiety around the carboxylic acid anchoring group, which arises from a considerably shorter π-spacer of CCT1A as shown in Figure 7. As a result, CCTT3A and CCT2PA dyes with longer π-conjugated spacers have more space to accommodate the donor moiety, allowing increased levels of dye uptake. For the same reason, CCTTnA had significantly lower levels of dye uptake on TiO_2 than TT2A. The chemisorption of all dyes onto the surface of TiO_2 films was confirmed by FTIR spectroscopic analysis, which showed feature absorption peaks of both the dyes

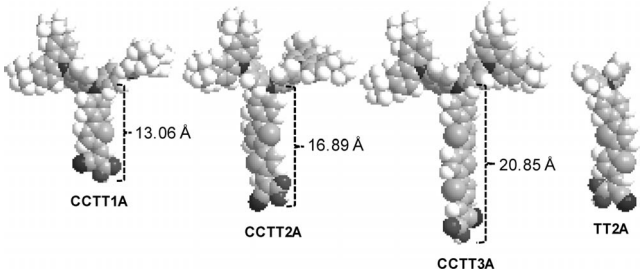

Figure 7. Space-filling molecular models of the optimized conformation of the dyes.

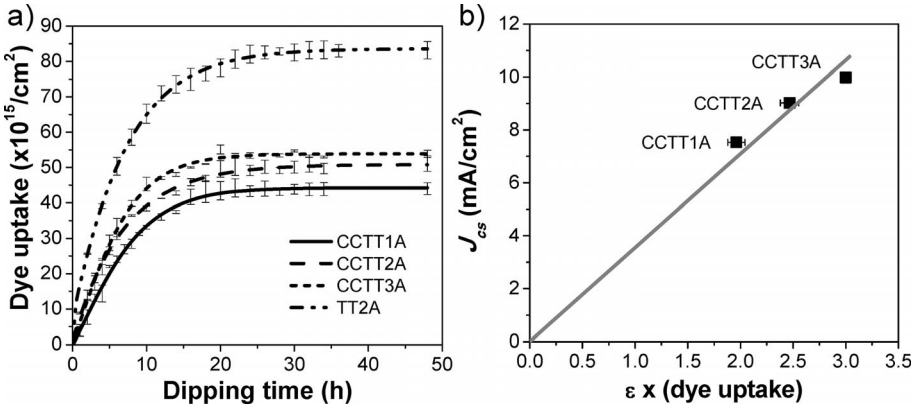

Figure 6. (a) The adsorption data for the dyes onto TiO_2 films measured over a period of 50 h at room temperature (line represents the numerical regression fit). (b) Linear relation between J_{sc} and $\varepsilon \times$(dye uptake). The linear regression line is $J_{sc} = 3.536$ [$\varepsilon \times$ (dye uptake)] with $R^2 = 0.995$.

Table 2. Performance parameters of DSSCs constructed using the dyes.

Dye	Dye uptake[a] ($\times 10^{15}$ molecule cm^{-2})	IPCE [%]	J_{sc} [mA cm^{-2}]	V_{oc} [V]	FF	η [%]	Cal. J_{sc}[b] [mA cm^{-2}]
CCTT1A	44.44 ± 1.95	70	7.53	0.72	0.69	3.70	6.67
CCTT2A	50.65 ± 1.81	80	9.02	0.71	0.68	4.34	8.76
CCTT3A	53.90 ± 0.50	76	9.98	0.70	0.67	4.62	9.91
TT2A	83.14 ± 2.43	69	6.89	0.69	0.71	3.38	6.81
N3	55.13 ± 1.02	68	12.18	0.65	0.66	5.20	11.43

[a] Obtained from dye adsorption measurement. [b] Obtained from integration of the corresponding IPCE spectra.

and TiO_2 at 2965 (C–H), 2207 (C≡N), 1611 (C=O), 1508 (C=C), 1365 (C=O), 1317, 1292, and 1226 cm^{-1} (see the Supporting Information). The characteristic vibration modes of the carboxylate group, both symmetric (1365 cm^{-1}) and asymmetric (1611 cm^{-1}), of all dyes were identical and were similar to that reported for other dyes independent of the molecular volume.[32] This indicates that all dyes bind in the same way to the TiO_2, therefore, the difference in the observed performance can be directly related to the effect of molecular volume and how much dye is absorbed.

Photovoltaic Properties of CCTTnA

CCTTnA and TT2A dyes were used as sensitizers for dye-sensitized nanocrystalline anatase TiO_2 solar cells (DSSCs). Cells with an effective area of 0.25 cm^2 (0.5 cm × 0.5 cm) were fabricated with 11 μm (9.5 μm transparent + 1.5 μm scattering) thick TiO_2 working electrode, platinum (Pt) counter electrode, and an electrolyte composed of 0.03 M I_2/0.6 M LiI/0.1 M guanidinium thiocyanate/0.5 M *tert*-butylpyridine in a 15:85 (v/v) mixture of benzonitrile/acetonitrile solution. The reference cell with the same structure based on N3 dye as the sensitizer, was made for comparison. To assess photovoltaic performance, five cells were prepared and measured under the standard conditions. The corresponding current density-voltage (*J-V*) characteristics and the incident monochromatic photon-to-current conversion efficiency (IPCE) plots are shown in Figure 8, and the resulting photovoltaic parameters (average values) are summarized in Table 2. The IPCE spectra of CCTTnA-sensitized DSSCs plotted as a function of excitation wavelength were broadened and redshifted as the number of thiophene units in the molecule increased, which is coincident with the absorption spectra. The IPCE action spectra for DSSC based on CCTT2A were considerably redshifted in comparison with that of a DSSC with TT2A as a result of having additional donors in CCTT2A; which is consistent with the UV/Vis absorption spectra of the dye-loaded TiO_2 films. The photocurrent response of CCTT2A-sensitized DSSC also had a higher value, exceeding 76% between 435 and 504 nm, compared with the other dyes. The maximum IPCE (80%) occurred at 475 nm, which is higher than the IPCE values of both CCTT1A- (70%) and CCTT3A (76%)-sensitized DSSCs. This observation deviates from our expectation on the basis of the ε values of their absorption spectra, but is also observed in other types of organic dyes.[33] In all devices, we observed a decrease in the IPCE above 600 nm in the long-wavelength region that can be attributed to a decrease in the light-harvesting efficiency of these dyes. The slightly lower IPCE value of CCTT3A-sensitized DSSC compared with that of CCTT2A-sensitized DSSC is probably due to extended π-conjugation elongation of CCTT3A, which may lead to decreased electron-injection yield relative to that of the CCTT2A dye.[34] This suggests that the structural modification of the dyes strongly influences electron-injection and the collection efficiencies, which, in turn, has a significant effect on the IPCE and overall conversion efficiency (η) of the devices. Moreover, the IPCE values of all synthesized dyes were higher than that of the N3 dye due to the larger molar extinction coefficients of these dyes, however, the N3 dye showed a broader IPCE spectrum, which is consistent with its wider absorption spectrum.

Under continuous visible-light irradiation (AM 1.5G, 100 mW cm^{-2}), the CCTT3A-sensitized DSSC showed the highest η among these dyes and gave a short-circuit photocurrent density (J_{sc}) of 9.98 mA cm^{-2}, open-circuit voltage (V_{oc}) of 0.70 V, and fill factor (FF) of 0.67, corresponding to a η of 4.62%. The J_{sc} and η values of the DSSCs were in the order: CCTT3A (9.98 mA cm^{-2}, 4.62%) > CCTT2A (9.02 mA cm^{-2}, 4.34%) > CCTT1A (7.53 mA cm^{-2}, 3.70%) > TT2A (6.89 mA cm^{-2}, 3.38%). The measured J_{sc} values of these solar cells were also cross-checked with the J_{sc} values calculated from integration of their corresponding IPCE spectra (Cal. J_{sc}), thus supporting the reported efficiency, with the results being in agreement to within 5% (Table 2). The larger J_{sc} and η of the CCTT2A (2D-D-π-A)-sensitized solar cell compared with that of a solar cell based on TT2A (D-π-A) demonstrates the beneficial influence of the redshifted absorption spectrum of CCTT2A on TiO_2 film and the broadening of the IPCE spectrum of CCTT2A-sensitized solar cell. This could result from cascading electron transfer from the additional carbazole do-

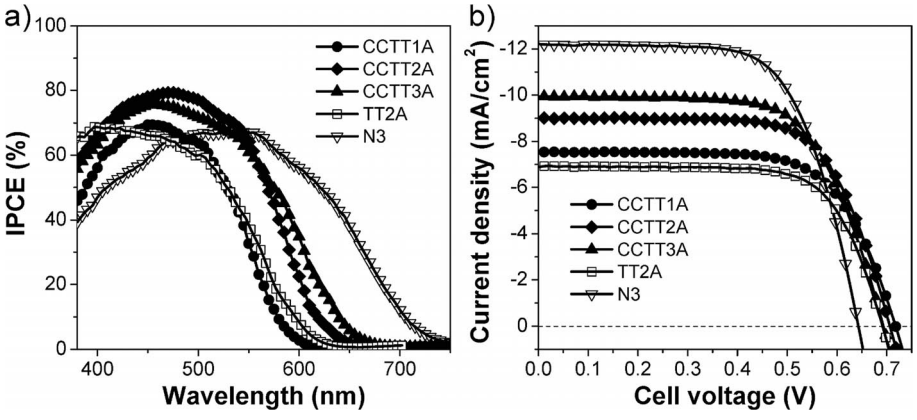

Figure 8. (a) IPCE plots and (b) *J-V* curves for the DSSCs.

nors to the acceptor moiety through the $S_0 \rightarrow S_2$ and $S_0 \rightarrow S_3$ transitions, as stated earlier. The use of *tert*-butyl groups as substituents on the peripheral carbazole might also play a role in shielding the TiO_2 surface from I^-/I_3^- in the electrolyte, thus reducing charge recombination or dark reaction, leading to the larger η of the device. In the CCTTnA dye series, the superior solar cell performance (highest η and J_{sc}) of the CCTT3A-sensitized DSSC could be rationalized by the redshifted absorption spectrum and broader IPCE response. Whereas the lower efficiency of the CCTT1A-based cell could be attributed to both the poorer spectral response and the lower dye content on TiO_2 film. The efficiency of CCTT3A-sensitized DSSC reaches 89% of the reference N3-based cell (η = 5.20%). Interestingly, the efficiency of the CCTT1A-based cell can also reach more than 71% that of the N3-based cell, even though the CCTT1A dye has a lower IPCE value and narrower IPCE spectrum than those of both CCTT2A and CCTT3A.

The ε value (in $mM^{-1}cm^{-1}$) multiplied by dye uptake (in $mol\,cm^{-2}$) makes a dimensionless value that corresponds to the absorbance of optical spectra. For the present dyes, these $\varepsilon \times$ (dye uptake) values showed excellent linear correlation to the observed J_{sc}, as shown in Figure 6 (b), for which the intercept was approximately zero (the zero intercept implies that no current density is observed for zero absorbance). This linear correlation holds true when the J_{sc} is determined only by the absorbance of photons. The length of the thiophene chain does not affect the mechanism of injection, charge separation, or charge recombination, but controls J_{sc} through ε and dye uptake efficiency. This length independence of the injection mechanism strongly suggests the direct injection mechanism for CCTTnA because such a mechanism may not explicitly involve the electronic states of the thiophene units.

Conclusions

We have developed a series of novel 2D-D-π-A-type organic sensitizers, namely CCTTnA, using bis(3,6-di-*tert*-butylcarbazol-9-ylphenyl)aniline as the electron-donor moiety (2D-D), oligothiophene segments as π-conjugated spacers (π), and cyanoacrylic acid as the electron acceptor (A). The study demonstrates the effect of the π-spacer length on controlling optical and photovoltaic properties. These dyes exhibit high thermal and electrochemical stability, which can enhance the stability of the solar cell. DSSCs constructed using these dyes as sensitizers exhibit efficiencies ranging from 3.7 to 4.62% under visible-light irradiation. The best performance among these dyes was found in CCTT3A, which shows a J_{sc} value of 9.98 $mA\,cm^{-2}$, V_{oc} value of 0.70, and FF value of 0.67, which correspond to a η of 4.62% (89% of the reference N3-based cell). The theoretical, optical, and electrochemical cell performance studies suggest that this type of donor architecture (2D-D) has a beneficial influence, with a redshifted absorption spectrum of the dye in solution and dye adsorbed on TiO_2 film, and a broadening of the IPCE spectrum of the solar cell. The DSSCs based on 2D-D-π-A-type dyes show larger J_{sc} and η compared with those of a solar cell based on a D-π-A dye. This work suggests that the organic dyes based on this 2D-D-π-A-type molecular architecture are promising candidates for the fabrication of DSSCs with improved performance. Moreover, structural modifications of these dyes to increase the molar extinction coefficient and further redshift the absorption spectrum is anticipated to give even better performance.

Experimental Section

Materials and Instruments: All reagents were purchased from Aldrich, Acros or Fluka, and used without further purification. All solvents were supplied by Thai companies and used without further distillation. THF was heated to reflux with sodium and benzophenone, and distilled prior to use. CH_2Cl_2 for electrochemical measurements was washed with conc. H_2SO_4 and distilled twice from calcium hydride. Chromatographic separations were carried out on silica gel Merck Silica gel 60 (0.0630–0.200 mm). 3,6-Di-*tert*-butylcarbazole (**1**) was prepared by adopting a literature procedure.[35]

^1H and ^{13}C NMR spectra were recorded with a Bruker AVANCE 300 MHz spectrometer with TMS as the internal reference using $CDCl_3$ or $CDCl_3$/[D_6]DMSO as solvents. IR spectra were measured with a Perkin–Elmer FTIR spectroscopy spectrum RXI spectrometer as KBr discs. UV/Vis spectra were recorded as dilute solutions in spectroscopic grade CH_2Cl_2 with a Perkin–Elmer UV Lambda 25 spectrometer. Diffuse reflectance spectra of the dye-sensitized TiO_2 were performed at room temperature with a Shimadzu UV-3101 spectrophotometer; barium sulfate was used as a standard. The measured reflectance spectra were then converted into absorption spectra by the Kubelka-Munk method. Steady-state fluorescence measurements were performed with a Jobin Yvon Fluoro-Max 2 fluorescence spectrometer with a slit width of 5 nm (for both excitation and emission slits). Lifetime measurements were performed by using subpicosecond laser based time-correlated single photon counting (TCSPC) with apparatus described by Landgraf including LED 450 nm, blue additive (BA) excitation filter and long pass filter 550 nm.[36] Ludox (colloidal silica) was used as scattering solution. All measurements were carried out in CH_2Cl_2 at 25 °C and deaerated with N_2 gas for 5 min before measuring. Thermal gravimetric analyses (TGA) were performed with a Rigaku TG-DTA 8120 thermal analyzer with a heating rate of 10 °C/min under an N_2 atmosphere. CV measurements were carried out with an Autolab potentiostat PGSTAT 12 with a three electrode system (platinum counter electrode, glassy carbon working electrode, and Ag/Ag^+ reference electrode) at a scan rate of 50 mV/s in CH_2Cl_2 under an argon atmosphere. The concentration of analytical materials and tetrabutylammonium hexafluorophosphate ($n$$Bu_4NPF_6$) were 1×10^{-3} M and 0.1 M, respectively. Melting points were measured with an Electrothermal IA 9100 series digital melting point instrument and are uncorrected. HRMS analysis was performed by the Mass Spectrometry Unit, Mahidol University, Thailand.

Dye Adsorption Measurements: The absorption spectra of the initial dye solution ($2.6–2.7 \times 10^{-5}$ M) in CH_2Cl_2 were measured with a Shimazu MultiSpec-1501 spectrophotometer. The TiO_2 substrates with an active area of 0.25 cm^2 (0.5 cm × 0.5 cm), prepared in the same manner as the substrate used for fabrication of DSSCs, were baked at 450 °C for 30 min and allowed to cool to 70–80 °C for before immersion into the dye solution in a screw cap quartz cuvette (1 cm × 1 cm). The absorption changes were monitored

hourly for 6 h and then very 2 h for 50 h. The amount of dye uptake was calculated from the calibration plot of known dye concentration. The chemisorption of all dyes onto TiO_2 film was characterized with a Perkin–Elmer FTIR spectroscopy spectrum RXI spectrometer.

Fabrication and Characterization of DSSCs. Device Fabrication: The photoanodes composed of nanocrystalline TiO_2 were prepared by using a previously reported procedure.[37] Fluorine-doped SnO_2 (FTO) conducting glasses (8 Ω/sq, TCO30-8, Solaronix) were used for transparent conducting electrodes. The double nanostructure thick film (ca. 11 μm thickness) consisting of transparent (Ti-Nanoxide 20T/SP, Solaronix) and scattering (Ti-Nanoxide R/SP, Solaronix) TiO_2 layers were screen-printed on $TiCl_4$-treated FTO. The thickness of the TiO_2 film was controlled by selection of screen mesh size and repetition of printing. Prior to dye sensitization, TiO_2 electrodes with cell geometry of $0.5 \times 0.5\ cm^2$ were treated with an aqueous solution of 4×10^{-2} M $TiCl_4$ at 70 °C in a water-saturated atmosphere, heated to 450 °C for 30 min and then cooled to 80 °C. The TiO_2 electrodes were immersed in the dye solution (3×10^{-4} M N3 in ethanol, and 5×10^{-4} M organic dyes in CH_2Cl_2) in the dark at room temperature for 30 h to stain the dye onto the TiO_2 surfaces. Excess dye was removed by rinsing with appropriate solvent. To ensure maximum dye adsorbed on the TiO_2 film, higher dyes concentration (> 10 fold) than that used for dye adsorption experiment was used. The Pt counter electrode was prepared on a predrilled TCO30-8 FTO glass (Solaronix) by thermal decomposition of 7×10^{-3} M [H_2PtCl_6] in 2-propanol solution at 385 °C. The dye-adsorbed TiO_2 photoanode and Pt counter electrode were assembled into a sealed cell by heating a gasket Meltonix 1170–25 film (25 μm thickness, Solaronix) as a spacer between the electrodes. An electrolyte solution of 0.6 M LiI, 0.03 M I_2, 0.1 M guanidinium thiocyanate, and 0.5 M *tert*-butylpyridine in 15:85 (v/v) mixture of benzonitrile and acetonitrile was filled through the predrilled hole by vacuum backfilling. The hole was capped by using hot-melt sealing film (Meltonix 1170–25, 25 μm thickness, Solaronix) and a thin glass cover. Finally, Schotch 3M conducting tape and silver paint (SPI supplies) were coated on the electrodes to enhance the electric contact. For each dye, five devices were fabricated and measured for consistency and the averaged cell data was reported. The reference cells with the same device configuration based on N3 dye as the sensitizer were also fabricated for comparison.

Device Characterization: The current density–voltage of the DSSCs was measured with a Keithley 2400 source meter unit in a 4-terminal sense configuration. The data were averaged from forward and backward scans with a bias step and a delay time of 10 mV and 40 ms, respectively, according to the method of Koidea and Han.[38] Simulated sunlight was provided by a Newport sun simulator 96000 equipped with an AM 1.5G filter. To minimize error, the irradiation intensity of 100 mW cm^{-2} was approximated with a calibrated BS-520 Si photodiode (Bunnkoukeiki Co., Ltd., Japan), which has a spectral response very similar to that of the DSSCs. The spectral output of the lamp was also matched to the standard AM 1.5G solar spectrum in the region of 350–750 nm with the aid of a KG-5 filter, with a spectral mismatch of less than 2%, as reported by Yanagida et al.[39] The IPCE of the device under short-circuit conditions were measured with an Oriel 150W Xe lamp fitted with a CornerstoneTM 130 1/8 m monochromator as a monochromatic light source, a Newport 818-UV silicon photodiode as power density calibration and a Keithley 6485 picoammeter. All measurements were performed by using a black plastic mask with an aperture area of 0.180 cm^2 and no mismatch correction for the efficiency conversion data.

Quantum Chemical Calculation: Ground-state geometries were fully optimized at the DFT level with the B3LYP hybrid functional. All optimizations were calculated without any symmetry constraints using the 6-31G(d,p) basis set with the Gaussian09 software package.[27]

Tris(4-iodophenyl)amine (2): A mixture of triphenylamine (9.8 g, 40 mmol), KI (14.6 g, 88 mmol), and KIO_3 (9.4 g, 44 mmol) in glacial acetic acid (300 mL) was heated at 110 °C for 6 h. The mixture was cooled and the formed precipitated was collected by suction filtration. The crude product was thoroughly washed with water (200 mL), and the solid was dissolved in CH_2Cl_2 (200 mL) and consecutively washed with water (2 × 100 mL), aqueous $NaHCO_3$ (2 × 100 mL), and brine solution (100 mL), dried with anhydrous Na_2SO_4, and filtered. After solvent evaporation, the pure compound (22.4 g, 90%) was obtained by recrystallization from a mixture of CH_2Cl_2/MeOH as a light-gray solid (m.p. 178–179 °C). FTIR (KBr): $\tilde{\nu}$ = 3056, 1574, 1482, 1311, 1284, 1004, 814 cm^{-1}. ^{1}H NMR (300 MHz, $CDCl_3$): δ = 7.52 (s, 6 H), 6.79 (s, 6 H) ppm. ^{13}C NMR (75 MHz, $CDCl_3$): δ = 146.0, 138.5, 126.0, 86.6 ppm. HRMS: *m*/*z* calcd. for $C_{18}H_{12}I_3N$ [MH^+] 622.8104; found 623.8187.

***N*,*N*-Bis[4-(3,6-di-*tert*-butylcarbazol-9-yl)phenyl]-4-iodoaniline (3):** A mixture of **2** (3.0 g, 4.8 mmol), **1** (2.7 g, 9.6 mmol), CuI (0.9 g, 4.8 mmol), K_3PO_4 (3.3 g, 24.1 mmol), and (±)-*trans*-1,2-diaminocyclohexane (0.6 mL, 4.8 mmol) in toluene (60 mL) was degassed with N_2 for 5 min and then heated at reflux under an N_2 atmosphere for 24 h. After cooling, the solid residue was filtered out and washed with CH_2Cl_2 (50 mL). The organic filtrate was washed with water (2 × 100 mL) and brine (100 mL), dried with anhydrous Na_2SO_4, and the solvents evaporated to dryness. Purification by silica gel column chromatography (CH_2Cl_2/hexane, 1:9) gave **3** (1.9 g, 44%) as a light-gray solid (m.p. > 250 °C). FTIR (KBr): $\tilde{\nu}$ = 3042, 2955, 1507, 1483, 1312, 1295, 1262, 810 cm^{-1}. ^{1}H NMR (300 MHz, $CDCl_3$): δ = 8.37 (s, 4 H), 7.80 (d, *J* = 7.2 Hz, 2 H), 7.50–7.68 (m, 16 H), 7.20 (d, *J* = 7.2 Hz, 2 H), 1.67 (s, 36 H) ppm. ^{13}C NMR (75 MHz, $CDCl_3$): δ = 147.2, 145.9, 145.6, 142.6, 139.4, 133.3, 130.9, 128.7, 127.8, 126.8, 125.3, 124.5, 123.6, 123.3, 122.7, 116.3, 110.8, 109.2, 34.8, 32.0 ppm. HRMS: *m*/*z* calcd. for $C_{58}H_{60}IN_3$ [MH^+] 925.3832; found 926.3902.

***N*,*N*-Bis[4-(3,6-di-*tert*-butylcarbazol-9-yl)phenyl]-4-(thiophen-2-yl)-aniline (4):** A mixture of **3** (2.0 g, 1.9 mmol), 2-thiopheneboronic acid (0.27 g, 1.9 mmol), [$Pd(PPh_3)_4$] (0.05 g, 0.04 mmol), aqueous 2 M Na_2CO_3 (16 mL) in THF (40 mL) was degassed with N_2 for 5 min and then heated at reflux under N_2 atmosphere for 24 h. After cooling, CH_2Cl_2 (100 mL) was added and the organic layer was washed with water (2 × 100 mL) and brine solution (100 mL), dried with anhydrous Na_2SO_4, filtered, and the solvents evaporated to dryness. Purification by silica gel column chromatography (CH_2Cl_2/hexane, 1:9) gave **4** (1.07 g, 63%) as a light-yellow solid (m.p. > 250 °C). FTIR (KBr): $\tilde{\nu}$ = 3041, 2958, 1507, 1473, 1316, 1294, 1262, 809 cm^{-1}. ^{1}H NMR (300 MHz, $CDCl_3$): δ = 8.11 (d, *J* = 5.4 Hz, 4 H), 7.59 (s, 2 H), 7.24–7.48 (m, 20 H), 7.05 (s, 1 H), 1.40 (s, 36 H) ppm. ^{13}C NMR (75 MHz, $CDCl_3$): δ = 146.6, 145.9, 143.6, 142.7, 139.1, 132.7, 129.5, 128.5, 127.7, 121.1, 125.2, 124.9, 123.8, 123.1, 116.5, 109.5, 34.8, 32.2 ppm. HRMS: *m*/*z* calcd. for $C_{62}H_{63}N_3S$ [MH^+] 881.4743; found 882.4819.

4-(5-Bromothiophen-2-yl)-*N*,*N*-bis[4-(3,6-di-*tert*-butylcarbazol-9-yl)-phenyl]aniline (5): *N*-Bromosuccinimide (0.35 g, 2.0 mmol) was added in small portions to a solution of **4** (1.7 g, 1.9 mmol) in THF (30 mL). The mixture was stirred at room temperature under N_2 for a further 1 h. Water (30 mL) and CH_2Cl_2 (100 mL) were added, and the organic phase was separated, washed with water (2 ×

100 mL), brine (100 mL), dried with anhydrous Na_2SO_4, filtered, and the solvents were removed to dryness. Purification by silica gel column chromatography (CH_2Cl_2/hexane, 1:9) gave the brominated product (1.5 g, 91%) as a light-yellow solid (m.p. > 250 °C). FTIR (KBr): $\tilde{\nu}$ = 3041, 2959, 1507, 1316, 1294, 1263, 809 cm^{-1}. ^1H NMR (300 MHz, $CDCl_3$): δ = 8.15 (d, J = 1.2 Hz, 4 H), 7.26–7.52 (m, 21 H), 7.03 (s, 1 H), 1.48 (s, 36 H) ppm. ^{13}C NMR (75 MHz, $CDCl_3$): δ = 147.3, 145.7, 142.9, 139.3, 138.5, 133.4, 127.7, 126.2, 125.2, 123.6, 123.3, 116.3, 109.2, 86.3, 34.7, 32.0 ppm. HRMS: m/z calcd. for $C_{62}H_{62}BrN_3S$ [MH^+] 959.3848; found 960.3908.

4-([2,2′-Bithiophen]-5-yl)-*N*,*N*-bis[4-(3,6-di-*tert*-butylcarbazol-9-yl)phenyl]aniline (6): Compound **6** (1.8 g, 63%) was prepared from **5** by using a similar method to that described above for **4** and obtained as a light-yellow-green solid (m.p. > 250 °C). FTIR (KBr): $\tilde{\nu}$ = 3041, 2953, 1507, 1316, 1293, 1262, 808 cm^{-1}. ^1H NMR (300 MHz, $CDCl_3$): δ = 8.16 (s, 4 H), 7.04–7.62 (m, 25 H), 1.48 (s, 36 H) ppm. ^{13}C NMR (75 MHz, $CDCl_3$): δ = 146.7, 145.9, 142.8, 139.4, 133.2, 129.2, 127.8, 127.7, 126.7,125.1, 124.6, 124.6, 124.6, 124.2,123.9, 123.3, 123.2, 116.2, 109.2, 34.8, 32.0 ppm. HRMS: m/z calcd. for $C_{66}H_{65}N_3S_2$ [MH^+] 963.4620; found 964.4637.

4-(5′-Bromo-[2,2′-bithiophen]-5-yl)-*N*,*N*-bis[4-(3,6-di-*tert*-butylcarbazol-9-yl)phenyl]aniline (7): Compound **7** (1.3 g, 87%) was prepared from **6** by using a similar method to that described above for **5** and obtained as a yellow-green solid (m.p. > 250 °C). FTIR (KBr): $\tilde{\nu}$ = 3041, 2959, 1507, 1318, 1294, 1263, 808 cm^{-1}. ^1H NMR (300 MHz, $CDCl_3$): δ = 8.16 (s, 4 H), 7.26–7.60 (m, 21 H), 7.18 (d, J = 3.6 Hz, 1 H), 7.09 (d, J = 3.9 Hz, 1 H), 6.98 (d, J = 3.6 Hz, 1 H), 6.94 (d, J = 3.9 Hz, 1 H), 1.49 (s, 36 H) ppm. ^{13}C NMR (75 MHz, $CDCl_3$): δ = 147.0, 145.8, 143.3, 142.8, 139.3, 139.0, 135.0, 133.2, 130.6, 127.7, 126.8, 125.2, 124.9, 124.4, 123.5, 123.3, 123.1, 116.2, 109.2, 34.7, 32.0 ppm. HRMS: m/z calcd. for $C_{66}H_{64}BrN_3S_2$ [MH^+] 1041.3725; found 1042.3773.

5-(4-{Bis[4-(3,6-di-*tert*-butylcarbazol-9-yl)phenyl]amino}phenyl)thiophene-2-carbaldehyde (8): A mixture of **3** (1.5 g, 1.8 mmol), 5-formyl-2-thiopheneboronic acid (0.15 g, 1.1 mmol), [$Pd(PPh_3)_4$] (0.02 g, 0.01 mmol), and 2 M aq Na_2CO_3 (12 mL) in THF (25 mL) was degassed with N_2 for 5 min and then heated at reflux under N_2 atmosphere for 24 h. After cooling, CH_2Cl_2 (100 mL) was added and the organic layer was washed with water (2× 100 mL) and brine solution (100 mL), dried with anhydrous Na_2SO_4, filtered, and the solvents evaporated to dryness. Purification by silica gel column chromatography (CH_2Cl_2/hexane, 1:5) gave **8** (0.75 g, 75%) as a yellow solid (m.p. > 250 °C). FTIR (KBr): $\tilde{\nu}$ = 3042, 2958, 1670 (C=O), 1599, 1507, 1446, 1317, 1294, 1263, 808 cm^{-1}. ^1H NMR (300 MHz, $CDCl_3$): δ = 9.89 (s, 1 H), 8.17 (s, 4 H), 7.74 (d, J = 3.9 Hz, 1 H), 7.66 (d, J = 8.4 Hz, 2 H), 7.42–7.56 (m, 15 H), 7.37 (d, J = 3.8 Hz, 1 H), 7.30 (d, J = 8.1 Hz, 2 H), 1.49 (s, 36 H) ppm. ^{13}C NMR (75 MHz, $CDCl_3$): δ = 182.5, 154.1, 148.7, 145.4, 142.9, 141.7, 139.3, 137.5, 133.9, 127.8, 127.6, 127.3, 125.8, 123.6, 123.4, 123.4, 123.2, 116.2, 109.2, 34.7, 32.0 ppm. HRMS: m/z calcd. for $C_{63}H_{63}N_3OS$ [M^+] 909.4692; found 909.4761.

5′-(4-{Bis[4-(3,6-di-*tert*-butylcarbazol-9-yl)phenyl]amino}phenyl)-[2,2′-bithiophene]-5-carbaldehyde (9): Compound **9** (0.64, 70%) was prepared from **5** by using a similar method to that described above for **8**, as a yellow solid (m.p. > 250 °C). FTIR (KBr): $\tilde{\nu}$ = 3042, 2959, 1665 (C=O), 1601, 1507, 1456, 1318, 1294, 1263, 808 cm^{-1}. ^1H NMR (300 MHz, $CDCl_3$): δ = 9.87 (s, 1 H), 8.18 (d, J = 1.3 Hz, 4 H), 7.67 (d, J = 3.9 Hz, 1 H), 7.61 (d, J = 8.6 Hz, 2 H), 7.25–7.55 (m, 21 H), 1.50 (s, 36 H) ppm. ^{13}C NMR (75 MHz, $CDCl_3$): δ = 182.3, 147.7, 147.2, 145.9, 145.7, 142.8, 141.4, 139.3, 137.3, 134.5, 133.4, 128.2, 127.8, 127.2, 127.0, 125.4, 124.1, 123.8, 123.5, 123.3, 116.2, 109.2, 34.7, 32.0 ppm. HRMS: m/z calcd. for $C_{67}H_{65}N_3OS_2$ [M^+] 991.4569; found 991.4728.

5′′-(4-{Bis[4-(3,6-di-*tert*-butylcarbazol-9-yl)phenyl]amino}phenyl)-[2,2′:5′,2′′-terthiophene]-5-carbaldehyde (10): Compound **10** (0.72 g, 60%) was prepared from **7** by using a similar method to that described above for **8**, as an orange solid (m.p. > 250 °C). FTIR (KBr): $\tilde{\nu}$ = 3041, 2957, 1665 (C=O), 1601, 1508, 1460, 1317, 1294, 1262, 808 cm^{-1}. ^1H NMR (300 MHz, $CDCl_3$): δ = 9.88 (s, 1 H), 8.17 (d, J = 1.5 Hz, 4 H), 7.70 (d, J = 4.2 Hz, 1 H), 7.61 (d, J = 8.4 Hz, 2 H), 7.23–7.55 (m, 22 H), 7.17 (d, J = 3.9 Hz, 1 H), 1.50 (s, 36 H) ppm. ^{13}C NMR (75 MHz, $CDCl_3$): δ = 182.3, 147.2, 146.8, 145.8, 144.0, 142.8, 141.6, 139.3, 139.3, 137.2, 135.0, 134.3, 133.3, 128.7, 127.7, 126.9, 125.5, 124.3 124.0, 123.5, 123.3, 116.2, 109.2, 34.7, 32.0 ppm. HRMS: m/z calcd. for $C_{71}H_{67}N_3OS_3$ [MH^+] 1073.4446; found 1074.4470.

2,2′-Bithiophene-5-carbaldehyde (11): Compound **11** (2.05 g, 89%) was prepared from 2-thiopheneboronic acid and 5-formyl-2-bromothiophene by using a similar method to that described above for **8**, as a light-yellow solid. FTIR (KBr): $\tilde{\nu}$ = 3409, 1649 (C=O), 1048, 798 cm^{-1}. ^1H NMR (300 MHz, $CDCl_3$): δ = 9.86 (s, 1 H), 7.66 (d, J = 3.9 Hz, 1 H), 7.35 (d, J = 4.4 Hz, 1 H), 7.25 (d, J = 3.9 Hz, 1 H), 7.08 (t, J = 4.4 Hz, 1 H) ppm. ^{13}C NMR (75 MHz, $CDCl_3$): δ = 182.52, 147.17, 141.74, 137.29, 136.05, 128.37, 127.10, 126.16, 124.27 ppm. HRMS: m/z calcd. for $C_9H_6OS_2$ [M^+] 193.9860; found 193.9755.

5′-Iodo-2,2′-bithiophene-5-carbaldehyde (12): *N*-Iodosuccinimide (2.45 g, 10.89 mmol) was added in small portions to a solution of **11** (1.76 g, 9.07 mmol) in THF/CH_3COOH (30/30 mL). The mixture was stirred at room temperature under N_2 for a further 1 h. Water (30 mL) and CH_2Cl_2 (100 mL) were added, and the organic phase was separated, washed with water (2× 100 mL), brine (100 mL), dried with anhydrous Na_2SO_4, filtered, and the solvents were removed to dryness. Purification by silica gel column chromatography (CH_2Cl_2/hexane, 1:9) gave the iodinated product (2.40 g, 83%) as a yellow solid. FTIR (KBr): $\tilde{\nu}$ = 3409, 1635 (C=O), 1613, 1048, 617 cm^{-1}. ^1H NMR (300 MHz, $CDCl_3$): δ = 9.87 (s, 1 H), 7.66 (d, J = 3.9 Hz, 1 H), 7.22 (d, J = 3.8 Hz, 1 H), 7.19 (d, J = 3.9 Hz, 1 H), 7.02 (d, J = 3.8 Hz, 1 H) ppm. ^{13}C NMR (75 MHz, $CDCl_3$): δ = 182.50, 145.59, 142.07, 141.88, 138.19, 137.12, 127.32, 124.57, 75.38 ppm. HRMS: m/z calcd. for $C_9H_5IOS_2$ [M^+] 319.8826; found 319.8811.

5′-[4-(Diphenylamino)phenyl]-2,2′-bithiophene-5-carbaldehyde (13): Compound **13** (0.71 g, 82%) was prepared from **12** and 4-(diphenylamino)phenylboronic acid by using a similar method to that described above for **8**, as an orange solid. FTIR (KBr): $\tilde{\nu}$ = 3045, 1671 (C=O), 1599, 1511, 1441, 1319, 1290, 1260, 807 cm^{-1}. ^1H NMR (300 MHz, $CDCl_3$): δ = 9.85 (s, 1 H), 7.66 (d, J = 3.6 Hz, 1 H), 7.45 (d, J = 7.5 Hz, 2 H), 7.24–7.31 (m, 6 H), 7.06–7.18 (m, 9 H) ppm. ^{13}C NMR (75 MHz, $CDCl_3$): δ = 182.37, 148.07, 147.44, 147.46, 146.29, 141.30, 137.41, 134.08, 129.41, 127.24, 127.10, 126.63, 124.83, 123.74, 123.48, 123.19, 123.14, 29.71 ppm. HRMS: m/z calcd. for $C_{27}H_{19}NOS_2$ [M^+] 437.0908; found 437.0915.

(*E*)-3-[5-(4-{Bis[4-(3,6-di-*tert*-butylcarbazol-9-yl)phenyl]amino}-phenyl)thiophen-2-yl]-2-cyanoacrylic Acid (CCTT1A): A mixture of **8** (0.3 g, 0.3 mmol), cyanoacetic acid (0.038 g, 0.4 mmol) and piperidine (2 drops) in chloroform (20 mL) was degassed with N_2 for 5 min and then heated at reflux under N_2 atmosphere for 18 h. After cooling, the reaction was quenched with water (5 mL) and extracted with CH_2Cl_2 (2× 50 mL). The combined organic layer was washed with water (2× 50 mL) and brine (50 mL), dried with anhydrous Na_2SO_4, filtered, and the solvents evaporated to dryness. Purification by silica gel column chromatography (MeOH/

CH_2Cl_2, 2:98) afforded the product (0.16 g, 58%) as an orange solid (m.p. > 250 °C). FTIR (KBr): $\tilde{\nu}$ = 3422 (O–H), 3042, 2958, 2214 (C≡N), 1582 (C=O), 1508, 1316, 1294, 1263, 808 cm^{-1}. ^1H NMR (300 MHz, $CDCl_3$/[D_6]DMSO): δ = 8.28 (s, 4 H), 8.17 (s, 1 H), 7.75 (d, J = 8.4 Hz, 3 H), 7.61 (d, J = 8.4 Hz, 5 H), 7.23–7.55 (m, 12 H), 7.27 (d, J = 8.4 Hz, 2 H), 1.41 (s, 36 H) ppm. ^{13}C NMR (75 MHz, $CDCl_3$/[D_6]DMSO): δ = 164.3, 150.1, 148.0, 145.5, 142.8, 139.0, 138.0, 135.5, 133.2, 127.9, 127.8, 125.9, 124.2 124.0, 123.5, 123.3, 116.8, 109.6, 34.9, 32.2 ppm. HRMS: *m*/*z* calcd. for $C_{66}H_{64}N_4O_2S$ [M^+] 976.4750; found 976.7170.

(*E*)-3-[5′-(4-{Bis[4-(3,6-di-*tert*-butylcarbazol-9-yl)phenyl]amino}-phenyl)-(2,2′-bithiophen)-5-yl]-2-cyanoacrylic Acid (CCTT2A): Compound CCTT2A (0.12 g, 57%) was prepared from **9** by using a similar method to that described above for CCTT1A, as a red solid (m.p. > 250 °C). FTIR (KBr): $\tilde{\nu}$ = 3422 (O–H), 3042, 2958, 2211 (C≡N), 1610 (C=O), 1508, 1363, 1317, 1294, 1263, 809 cm^{-1}. ^1H NMR (300 MHz, $CDCl_3$/[D_6]DMSO): δ = 8.27 (d, J = 1.2 Hz, 4 H), 8.00 (s, 1 H), 7.73 (d, J = 8.4 Hz, 2 H), 7.35–7.63 (m, 20 H), 7.26 (d, J = 8.4 Hz, 2 H), 1.40 (s, 36 H) ppm. ^{13}C NMR (75 MHz, $CDCl_3$/[D_6]DMSO): δ = 163.8, 147.2, 145.7, 144.1, 142.8, 141.7, 139.0, 136.1, 134.7, 133.0, 128.4, 127.9, 127.2, 125.6, 124.7, 124.5, 124.0, 123.1, 119.6, 116.8, 109.6, 34.8, 32.2 ppm. HRMS: *m*/*z* calcd. for $C_{70}H_{66}N_4O_2S_2$ [MH^+] 1058.4627; found 1059.3502.

(*E*)-3-[5′′-(4-{Bis[4-(3,6-di-*tert*-butylcarbazol-9-yl)phenyl]amino}-phenyl)-(2,2′:5′,2′′-terthiophen)-5-yl]-2-cyanoacrylic Acid (CCTT3A): Compound CCTT3A (0.19 g, 48%) was prepared from **10** by using a similar method to that described above for CCTT1A, as a dark-red solid (m.p. > 250 °C). FTIR (KBr): $\tilde{\nu}$ = 3419 (O–H), 3042, 2960, 2213 (C≡N), 1609 (C=O), 1508, 1364, 1317, 1294, 1263, 808 cm^{-1}. ^1H NMR (300 MHz, $CDCl_3$/[D_6]DMSO): δ = 8.27 (s, 4 H), 8.05 (s, 1 H), 7.70 (d, J = 8.4 Hz, 2 H), 7.64 (d, J = 4.2 Hz, 1 H), 7.57 (d, J = 8.4 Hz, 4 H), 7.32–7.47 (m, 17 H), 7.25 (d, J = 8.4 Hz, 2 H), 1.39 (s, 36 H) ppm. ^{13}C NMR (75 MHz, $CDCl_3$/[D_6]DMSO): δ = 164.5, 147.0, 145.7, 143.2, 142.8, 142.3, 141.8, 139.0, 137.7, 137.2, 135.8, 134.8, 134.5, 132.9, 128.5, 127.8, 127.1, 127.0, 126.2, 125.5, 125.3, 124.8, 124.4, 123.9, 123.1, 118.9, 116.7, 109.5, 34.9, 32.2 ppm. HRMS: *m*/*z* calcd. for $C_{74}H_{68}N_4O_2S_3$ [M^+] 1140.4504; found 1140.5029.

(*E*)-3-{5′-[4-(Diphenylamino)phenyl]-2,2′-bithiophen-5-yl}-2-cyanoacrylic Acid (TT2A): Compound TT2A (0.20 g, 79%) was prepared from **13** by using a similar method to that described above for CCTT1A, as a red-orange solid (m.p. > 250 °C). FTIR (KBr): $\tilde{\nu}$ = 3418 (O–H), 3044, 2964, 2211 (C≡N), 1611 (C=O), 1512, 1364, 1315, 1284, 1260, 808 cm^{-1}. ^1H NMR (300 MHz, [D_6]DMSO): δ = 8.00 (s, 1 H), 7.58–7.62 (m, 3 H), 7.40–7.45 (m, 3 H), 7.30–7.35 (m, 4 H), 7.04–7.10 (m, 6 H), 6.93 (d, J = 8.4 Hz, 2 H) ppm. ^{13}C NMR (75 MHz, [D_6]DMSO): δ = 147.72, 147.19, 144.32, 141.53, 140.20, 136.56, 136.18, 134.32, 130.15, 127.29, 127.19, 126.97, 124.96, 124.62, 124.55, 124.10, 123.13, 119.80 ppm. HRMS: *m*/*z* calcd. for $C_{30}H_{20}N_2O_2S_2$ [M^+] 504.0966; found 504.0983.

Supporting Information (see footnote on the first page of this article): Quantum chemical calculations, multiple CV scans, FTIR spectra, and UV/Vis absorption spectra of dyes adsorbed on TiO_2, and ^1H and ^{13}C NMR spectra of the dyes and intermediates.

Acknowledgments

This work was supported by the Thailand Research Fund (grant number RMU5080052), the Strategic Scholarships for Frontier Research Network for Research Groups (grant number CHE-RES-RG50) funded by the Office of the Higher Education Commission, Thailand, and the Electricity Generating Authority of Thailand (EGAT). The authors acknowledge scholarship support from the Royal Golden Jubilee (RGJ) Ph.D. Program and the Center of Excellence for Innovation in Chemistry (PERCH-CIC) to T. K., S. M., and N. J.

[1] B. O'Regan, M. Grätzel, *Nature* **1991**, *353*, 737–740.
[2] a) A. Hagfeldt, M. Grätzel, *Chem. Rev.* **1995**, *95*, 49–68; b) M. Grätzel, *Nature* **2001**, *414*, 338–344; c) Z. Ning, Y. Fu, H. Tian, *Energ. Environ. Sci.* **2010**, *3*, 1170–1181.
[3] M. A. Green, K. Emery, Y. Hishihir, W. Warta, *Prog. Phohovolt. Res. Appl.* **2011**, *19*, 84–92.
[4] a) M. K. Nazeeruddin, P. Péchy, T. Renouard, S. M. Zakeeruddin, R. Humphry-Baker, M. Grätzel, *J. Am. Chem. Soc.* **2001**, *123*, 1613–1624; b) F. Gao, Y. Wang, D. Shi, J. Zhang, M. Wang, X. Jing, R. Humphry-Baker, P. Wang, S. M. Zakeeruddin, M. Grätzel, *J. Am. Chem. Soc.* **2008**, *130*, 10720–10728; c) K.-J. Jiang, N. Masaki, J. Xia, S. Noda, S. Yanagida, *Chem. Commun.* **2006**, 2460–2462; d) M. Maestri, N. Armaroli, V. Balzani, E. C. Constable, A. M. W. Cargill Thompson, *Inorg. Chem.* **1995**, *34*, 2759–2767; e) C.-Y. Chen, J.-G. Chen, S.-J. Wu, J.-Y. Li, C.-G. Wu, K.-C. Ho, *Angew. Chem.* **2008**, *120*, 7452; *Angew. Chem. Int. Ed.* **2008**, *47*, 7342–7345.
[5] H. Tian, F. Meng, *Organic Photovoltaics: Mechanisms, Materials, and Devices* London, CRC, **2005**.
[6] a) W. Wu, J. Yang, J. Hua, J. Tang, L. Zhang, Y. Long, H. Tian, *J. Mater. Chem.* **2010**, *20*, 1772–1779; b) S. Qu, W. Wu, J. Hua, C. Kong, Y. Long, H. Tian, *J. Phys. Chem. C* **2010**, *114*, 1343–1349; c) L.-Y. Lin, C.-H. Tsai, K.-T. Wong, T.-W. Huang, L. Hsieh, S.-H. Liu, H.-W. Lin, C.-C. Wu, S.-H. Chou, S.-H. Chen, A.-I. Tsai, *J. Org. Chem.* **2010**, *75*, 4778–4785; d) G. Li, K. J. Jiang, Y. F. Li, S. L. Li, L. M. Yang, *J. Phys. Chem. C* **2008**, *112*, 11591–11599; e) Y. S. Chen, C. Li, Z. H. Zeng, W. B. Wang, X. S. Wang, B. W. Zhang, *J. Mater. Chem.* **2005**, *15*, 1654–1661; f) J. A. Mikroyannisdis, D. V. Tsagkournos, P. Balraju, G. D. Sharma, *J. Power Sources* **2011**, *196*, 4152–416; g) H. Imahori, T. Umeyama, S. Ito, *Acc. Chem. Res.* **2009**, *42*, 1809–1818.
[7] C.-L. Wang, Y.-C. Chang, C.-M. Lan, C.-F. Lo, E. W.-G. Dian, C.-Y. Lin, *Energ. Environ. Sci.* **2011**, *4*, 1788–1795.
[8] A. Mishra, M. K. R. Fischer, P. Bäuerle, *Angew. Chem.* **2009**, *121*, 2510; *Angew. Chem. Int. Ed.* **2009**, *48*, 2474–2499.
[9] a) A. Ehret, L. Stuhi, M. T. Spitler, *J. Phys. Chem. B* **2001**, *105*, 9960–9965; b) S. Tan, J. Zhai, H. Fang, T. Jiu, J. Ge, Y. Li, L. Jiang, D. Zhu, *Chem. Eur. J.* **2005**, *11*, 6272–6276; c) M. C. Gather, D. D. C. Bradley, *Adv. Funct. Mater.* **2007**, *17*, 479–48; d) K. Sayama, K. Hara, N. Mori, M. Satsuki, S. Suga, S. Tsukagoshi, Y. Abe, H. Sugihara, H. Arakawa, *Chem. Commun.* **2000**, 1173–1174.
[10] a) R. F. Fink, J. Seibt, V. Engel, M. Renz, M. Kaupp, S. Lochbrunner, H. M. Zhao, J. Pfister, F. Wurthner, B. Engels, *J. Am. Chem. Soc.* **2008**, *130*, 12858–12859; b) S. Tatay, S. A. Haque, B. O'Regan, J. R. Durrant, W. J. H. Verhees, J. M. Kroon, A. Vidal-Ferran, P. Gavina, E. Palomares, *J. Mater. Chem.* **2007**, *17*, 3037–3044.
[11] a) T. Kai, L. Mao, L. Yongkang, S. Zhe, X. Song, *Chin. J. Chem.* **2011**, *29*, 89–96; b) H. Chen, H. Huang, X. Huang, J. N. Clifford, A. Forneli, E. Palomares, X. Zheng, L. Zheng, X. Wang, P. Shen, B. Zhao, S. Tan, *J. Phys. Chem. C* **2010**, *114*, 3280–3286; c) Z. Ning, Q. Zhang, H. Pei, J. Luan, C. Lu, Y. Cui, H. Tian, *J. Phys. Chem. C* **2009**, *113*, 10307–10313; d) M. Velusamy, Y.-C. Hsu, J. T. Lin, C.-W. Chang, C.-P. Hsu, *Chem. Asian J.* **2010**, *5*, 87–96.
[12] a) S. Hwang, J. H. Lee, C. Park, H. Lee, C. Kim, C. Park, M.-H. Lee, W. Lee, J. Park, K. Kim, N.-G. Park, C. Kim, *Chem. Commun.* **2007**, 4887–4889; b) Z.-S. Wang, N. Koumura, Y.

Cui, M. Takahashi, H. Sekiguchi, A. Mori, T. Kubo, A. Furube, K. Hara, *Chem. Mater.* **2008**, *20*, 3993–4003.
[13] a) W. Xu, B. Peng, J. Chen, M. Liang, F. Cai, *J. Phys. Chem. C* **2008**, *112*, 874–880; b) Z. Ning, H. Tian, *Chem. Commun.* **2009**, 5483–5495.
[14] a) A. Thangthong, D. Meunmart, N. Prachumrak, S. Jungsuttiwong, T. Keawin, T. Sudyoadsuk, V. Promarak, *Chem. Commun.* **2011**, *47*, 7122–7124; b) V. Promarak, M. Ichikawa, T. Sudyoadsuk, S. Saengsuwan, S. Jungsuttiwong, T. Keawin, *Thin Solid Films* **2008**, *516*, 2881–2888; c) V. Promarak, M. Ichikawa, T. Sudyoadsuk, S. Saengsuwan, S. Jungsuttiwong, T. Keawin, *Synth. Met.* **2007**, *157*, 17–22.
[15] Y. J. Chang, T. J. Chow, *Tetrahedron* **2009**, *65*, 4726–4734.
[16] V. Promarak, M. Ichikawa, T. Sudyoadsuk, S. Saengsuwan, T. Keawin, *Opt. Mater.* **2007**, *30*, 364–369.
[17] V. Promarak, A. Punkvuang, T. Sudyoadsuk, S. Jungsuttiwong, S. Saengsuwan, T. Keawin, K. Sirithip, *Tetrahedron* **2007**, *63*, 8881–8890.
[18] P. Shen, Y. Liu, X. Huang, B. Zhao, N. Xiang, J. Fei, L. Liu, X. Wang, H. Huang, S. Tan, *Dyes Pigm.* **2009**, *83*, 187–197.
[19] H. M. Nguyen, D. N. Nguyen, N. Kim, *Adv. Nat. Sci. Nanosci. Nanotechnol.* **2010**, *1*, 025001.
[20] A. C. Khazriji, S. Hotchadani, S. Das, P. V. Kamat, *J. Phys. Chem. B* **1999**, *103*, 4693–4700.
[21] a) K. R. J. Thomas, Y. C. Hsu, J. T. Lin, K. M. Lee, K. C. Ho, C. H. Lai, Y. M. Cheng, P. T. Chou, *Chem. Mater.* **2008**, *20*, 1830–1840; b) M. Lu, M. Liang, H.-Y. Han, Z. Sun, S. Xue, *J. Phys. Chem. C* **2011**, *115*, 274–281.
[22] V. Promarak, A. Pankvuang, D. Meunmat, T. Sudyoadsuk, S. Saengsuwan, T. Keawin, *Tetrahedron Lett.* **2007**, *48*, 919–923.
[23] K. T. Kamtekar, C. Wang, S. Bettington, A. S. Batsanov, I. F. Perepichka, M. R. Bryce, J. H. Ahn, M. Rabinal, M. C. Petty, *J. Mater. Chem.* **2006**, *16*, 3823–3835.
[24] S. Haid, M. Marszalek, A. Mishra, M. Wielopolski, J. Teuscher, J.-E. Moser, R. Humphry-Baker, S. M. Zakeeruddin, M. Grätzel, P. Bäuerle, *Adv. Funct. Mater.* **2012**, *22*, 1291–1302.
[25] J.-J. Lee, M. M. Rahman, S. Sarker, D. Nath, *Advances in Composite Materials for Medicine and Nanotechnology*, *InTech* **2011**, 181–210.
[26] a) H. Choi, C. Baik, S. O. Kang, J. Ko, M.-S. Kang, M. K. Nazeeruddin, M. Grätzel, *Angew. Chem.* **2008**, *120*, 333; *Angew. Chem. Int. Ed.* **2008**, *47*, 327–330; b) S. Hwang, J. H. Lee, C. Park, H. Lee, C. Kim, C. Park, M.-H. Lee, W. Lee, J. Park, K. Kim, N.-G. Park, C. Kim, *Chem. Commun.* **2007**, 4887–4889; c) M.-S. Tsai, Y.-C. Hsu, J. T. Lin, H.-C. Chen, C.-P. Hsu, *J. Phys. Chem. C* **2007**, *111*, 18785–18793.
[27] M. J. Frisch, G. W. Trucks, H. B. Schlegel, G. E. Scuseria, M. A. Robb, J. R. Cheeseman, G. Scalmani, V. Barone, B. Mennucci, G. A. Petersson, H. Nakatsuji, M. Caricato, X. Li, H. P. Hratchian, A. F. Izmaylov, J. Bloino, G. Zheng, J. L. Sonnenberg, M. Hada, M. Ehara, K. Toyota, R. Fukuda, J. Hasegawa, M. Ishida, T. Nakajima, Y. Honda, O. Kitao, H. Nakai, T. Vreven, J. A. Montgomery Jr., J. E. Peralta, F. Ogliaro, M. Bearpark, J. J. Heyd, E. Brothers, K. N. Kudin, V. N. Staroverov, R. Kobayashi, J. Normand, K. Raghavachari, A. Rendell, J. C. Burant, S. S. Iyengar, J. Tomasi, M. Cossi, N. Rega, J. M. Millam, M. Klene, J. E. Knox, J. B. Cross, V. Bakken, C. Adamo, J. Jaramillo, R. Gomperts, R. E. Stratmann, O. Yazyev, A. J. Austin, R. Cammi, C. Pomelli, J. W. Ochterski, R. L. Martin, K. Morokuma, V. G. Zakrzewski, G. A. Voth, P. Salvador, J. J. Dannenberg, S. Dapprich, A. D. Daniels, O. Farkas, J. B. Foresman, J. V. Ortiz, J. Cioslowski, D. J. Fox, *Gaussian 09*, Revision A.1, Gaussian, Inc., Wallingford, CT, **2009**.
[28] Z. J. Ning, Y. C. Zhou, Q. Zhang, D. G. Ma, J. J. Zhang, H. Tian, *J. Photochem. Photobiol. A: Chem.* **2007**, *192*, 8–16.
[29] Y. Tachinaba, S. A. Haque, I. P. Mercer, J. R. Durrant, D. R. Klug, *J. Phys. Chem. B* **2000**, *104*, 1198–1205.
[30] B.-K. An, R. Mulherin, B. Langley, P. L. Burn, P. Meredith, *Org. Electron.* **2009**, *10*, 1356–1363.
[31] Z. Yaneva, B. Koumanova, *J. Colloid Interface Sci.* **2006**, *293*, 303–311.
[32] a) S. E. Ela, M. Marszalek, S. Tekoglu, M. Can, S. Icli, *Curr. Appl. Phys.* **2010**, *10*, 749–756; b) M. K. Nazeeruddin, R. Humphry-Baker, P. Liska, M. Grätzel, *J. Phys. Chem. B* **2003**, *107*, 8981–8987.
[33] K. D. Seo, H. M. Song, M. J. Lee, M. Pastore, C. Anselmi, F. D. Angelis, M. K. Nazeeruddin, M. Gräetzel, H. K. Kim, *Dyes Pigm.* **2011**, *90*, 304–310.
[34] K. Hara, Z. S. Wang, T. Sato, A. Furube, R. Katoh, H. Sugihara, Y. Dan-oh, C. Kasada, A. Shinpo, S. Suga, *J. Phys. Chem. B* **2005**, *109*, 15476–15482.
[35] T. Xu, R. Lu, X. Liu, X. Zheng, X. Qiu, Y. Zhao, *Org. Lett.* **2007**, *9*, 797–800.
[36] S. Landgraf, *Spectrochim. Acta Part A* **2001**, *57*, 2029–2048.
[37] D. P. Hagberg, J.-H. Yum, H. Lee, F. De Angelis, T. Marinado, K. M. Karlsson, R. Humphry-Baker, L. Sun, A. Hagfeldt, M. Grätzel, M. K. Nazeeruddin, *J. Am. Chem. Soc.* **2008**, *130*, 6259–6266.
[38] N. Koidea, L. Han, *Rev. Sci. Instrum.* **2004**, *75*, 2828–2831.
[39] S. Ito, H. Matsui, K. Okada, S. Kusano, T. Kitamura, Y. Wada, S. Yanagida, *Sol. Energy Mater. Sol. Cells* **2004**, *82*, 421–429.

Received: November 6, 2012
Published Online: March 13, 2013

